

Cite this article as: Li Zengde, Li Qing, Xie Haofeng, et al. Effect of Microstructure and Precipitate on Tensile Properties of V-5Cr-5Ti Alloy[J]. Rare Metal Materials and Engineering, 2022, 51(08): 2745-2753.

ARTICLE

# Effect of Microstructure and Precipitate on Tensile Properties of V-5Cr-5Ti Alloy

Li Zengde<sup>1,2</sup>, Li Qing<sup>1,2</sup>, Xie Haofeng<sup>1,2</sup>, Peng Lijun<sup>1,2</sup>, Yang Zhen<sup>1,2</sup>, Zhang Wenjing<sup>1,2</sup>, Huang Shuhui<sup>1,2</sup>, Zhang Ximin<sup>1,2</sup>, Huang Guojie<sup>1,2</sup>

<sup>1</sup> State Key Laboratory of Nonferrous Metals and Processes, GRINM Group Co., Ltd, Beijing 100088 China; <sup>2</sup> Nonferrous Metals Structural Materials Department, GRIMAT Engineering Institute Co., Ltd, Beijing 101104, China

**Abstract:** After homogenization, forging, cold rolling, and recrystallization of V-5Cr-5Ti alloy, universal testing machine, scanning electron microscopy, and transmission electron microscopy were used to study the effect of precipitates on the mechanical properties of the alloy and to estimate the strengthening effect. Results show that as-cast V-5Cr-5Ti alloy has a dendritic structure characterized by lamellar phase. After homogenization, the precipitates are transformed from a lamellar to a needle-like dendritic structure. The precipitates are broken into a short-bar or spherical phase during forging and cold rolling. The average tensile strength, yield strength, and elongation of the as-cast alloy are 505.0 MPa, 415.0 MPa, and 8.2%, respectively, with the brittle cleavage fracture as the dominant fracture mechanism. The fracture mechanism is transformed into a mixed fracturing mode of intergranular and quasi-dissociative fractures after homogenization. After 80% cold rolling and 1000 °C/1 h annealing, the average tensile strength, yield strength, and elongation of the alloy are 487.3 MPa, 382.7 MPa, and 26.2%. The alloy plasticity is greatly improved due to the refinement of the grain and precipitates. The fracture mechanism of the alloy after cold rolling and annealing is microporosity fracture. The precipitates enhance V-5Cr-5Ti alloy by Orowan strengthening mechanism. Taking the alloy after 80% cold rolling and annealing at 1000 °C/1 h as an example, the yield strength increment obtained by precipitate strengthening is about 50.1 MPa.

**Key words:** V-5Cr-5Ti alloy; microstructure; precipitate; tensile property; fracture mechanism; precipitation strengthening

As an important candidate structural material for fusion reactors, V-based alloy has low activation properties<sup>[1]</sup>, good high-temperature strength<sup>[2-5]</sup>, low-temperature toughness<sup>[6]</sup>, antineutron irradiation swelling<sup>[7-9]</sup>, and resistance to liquid metal corrosion<sup>[10,11]</sup>. Worldwide research on V-based materials is mainly focused on V-(4-5)Cr-(4-5)Ti alloys. In comparison with V-4Cr-4Ti alloy, V-5Cr-5Ti alloy has higher room-temperature/high-temperature strength due to higher contents of Cr and Ti elements. However, as the content of Cr element increases, the antineutron swelling performance of the alloy decreases. The resistance to liquid metal (Li or Li-Pd) corrosion increases with the increase in Ti element content<sup>[12]</sup>. China Academy of Engineering Physics has investigated the performance, including mechanical properties, welding properties, and corrosion resistance of V-5Cr-5Ti alloy<sup>[13-16]</sup>. This alloy has excellent comprehensive properties and is expected

to become a key material for China's nuclear industry.

The mechanical properties of V-base alloys have been studied in detail. Most research is focused on the effects of alloying elements, irradiation, and the precipitates on the mechanical properties<sup>[17-25]</sup>, whereas few are reported on the strengthening mechanism of V alloys. Chen et al<sup>[26]</sup> believed that Ti(CON) is precipitated during aging, showing an evident strengthening effect, but the alloy plasticity does not change significantly. Nishimura et al<sup>[27]</sup> concluded that the plasticity reduction caused by aging strengthening is within the tolerance range for engineering application of V alloys. Fu et al<sup>[4]</sup> emphasized that severe deterioration of V alloy precipitates occurs at the grain boundary during aging. Nano-sized precipitates can be obtained only through multiple thermal mechanical treatments, and the strengthening effect of the alloy is good.

Received date: August 22, 2021

Foundation item: National Natural Science Foundation of China (U1532262)

Corresponding author: Li Zengde, Ph. D., Professor, Nonferrous Metals Structural Materials Department, GRIMAT Engineering Institute Co., Ltd, Beijing 101104, P. R. China, Tel: 0086-10-60662686, E-mail: lizengde@grinm.com

Copyright © 2022, Northwest Institute for Nonferrous Metal Research. Published by Science Press. All rights reserved.

In the present study, the mechanical properties of V-5Cr-5Ti alloy were evaluated at room temperature via tensile test, and changes in the strength and plasticity of the alloy under different states were studied. Through microscopic observation, the influence of precipitates on the mechanical properties of V-5Cr-5Ti alloy was analyzed, and the strengthening effect of the precipitates was estimated.

## 1 Experiment

V-5Cr-5Ti alloy was prepared by vacuum melting of high-purity V, Cr, and Ti. The V-5Cr-5Ti alloy used in this work was processed by the following steps: homogenization annealing, hot forging, and cold rolling. The homogenization was conducted at 1200 °C for 3 h in a vacuum ( $< 2 \times 10^{-2}$  Pa). To prevent the oxidation of vanadium alloys and to avoid environmental pollution during the hot working process, vanadium alloys must be protected under a vacuum better than  $< 2 \times 10^{-2}$  Pa. The vacuum canning material comprised 3 mm thick 1Cr18Ni9Ti stainless steel. The canning billet was heated in a furnace at 1080 °C for 100 min and then die forged in 10000 kN forging hydraulic machine until ~50% of the height reduction. The thickness reduction was 40% and 80% for cold-rolling. Fig. 1 is the microstructure of as-cast V-5Cr-5Ti alloy. Table 1 shows their chemical composition of V-5Cr-5Ti alloy after hot forging.

Tensile samples were cut from as-cast V-5Cr-5Ti alloy, V-5Cr-5Ti alloy plates were subjected to homogenization, hot forging+1020 °C/1 h annealing and 40%, 80% cold rolling. Part of the cold-rolling sheet was subjected to recrystallization annealing at 1000 °C/1 h in a vacuum ( $< 2 \times 10^{-2}$  Pa). The V-5Cr-5Ti alloy was sampled along the rolling direction for tensile test, as shown in Fig. 2. The tensile test was conducted on an electronic universal testing machine with a gauge length of 20 mm and tensile rates of 0.5 mm/min before yield point and 2 mm/min after yield point.

The microstructure and tensile fracture morphology of V-5Cr-5Ti alloy were observed using scanning electron microscope (SEM, model JSM-7001F). The sample for microstructure observation was subjected to electrolytic

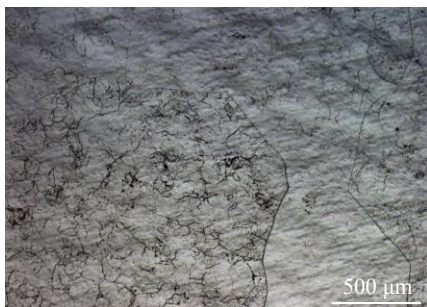


Fig.1 As-cast microstructure of V-5Cr-5Ti alloy

Table 1 Chemical composition of V-5Cr-5Ti alloy (wt%)

Cr	Ti	C	O	N	Al	Fe	V
4.86	4.98	0.0102	0.038	0.0037	0.041	0.026	Bal.

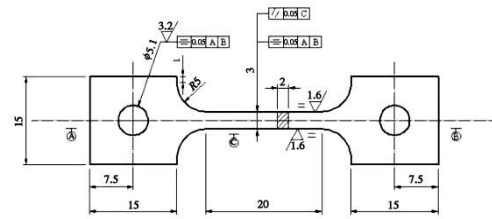


Fig.2 Drawing of the tensile test sample

etching with solution HF:H<sub>2</sub>O=1:10 (volume ratio) under a voltage of 15 V and current of 0.6~1.0 A for 30 s.

The microstructure of the precipitates of V-5Cr-5Ti alloy was analyzed using FEI Tecnai F20 field transmission electron microscope (TEM). The MTP double-electrolytic jet apparatus was adopted for sample preparation, with 5vol% H<sub>2</sub>SO<sub>4</sub>+95vol% CH<sub>3</sub>OH as electrolyte, under a voltage of 10 V and electric current of ~20 mA at -10 °C.

## 2 Results and Discussion

### 2.1 Microstructure

V-5Cr-5Ti alloy ingots were prepared via secondary vacuum electron beam melting. Microsegregation of the ingots easily occurs due to the high temperature of vacuum electron beam melting, fast cooling rate, poor fluidity, and thermal conductivity of the V-5Cr-5Ti alloy. Fig. 3 shows the as-cast microstructure of the V-5Cr-5Ti alloy. The grain size of the V-5Cr-5Ti alloy ingots is large, a large component segregation area exists in some grains, and the morphology of the alloy precipitates present a dendritic structure and small granular phase (Fig. 3a). The precipitates are stratified and stacked into a lamellar curve, with a lamella thickness of approximately 100 nm and width of 1~2 μm (Fig. 3b). After homogenization, the morphology of the precipitates changes from a lamellar to a needle-like dendritic structure (Fig. 3c). The needle-like phase is stacked into a dendritic structure via a certain orientation (parallel or vertical), as shown in Fig. 3d. The thickness of the needle-like phase is less than 100 nm, and the length is less than 4 μm.

After forging and 1020 °C/1 h annealing, the grain of V-5Cr-5Ti alloy is a type of equiaxial grain structure, with a grain size of approximately 80 μm. The precipitates are in zonal distribution (Fig. 4a). The precipitates mainly exist in the form of short-bar phases (~1 μm) and distributed irregularly at the grain boundary and surrounding area (Fig. 4b). Fig. 4c and 4d present the SEM images of 40% cold-rolled V-5Cr-5Ti alloy. The grains are stretched along the rolling direction, forming fibrous structures. The precipitates change into banded structures with rolling deformation, and most of precipitates are arranged along the rolling direction. The short-strip phases can be attained after cold rolling. Some small round phases are distributed sporadically in the matrix (Fig. 4d). Fig. 4e and 4f display the SEM images of 80% cold-rolled V-5Cr-5Ti alloy. The grains are stretched into a fibrous structure along the rolling direction. The precipitates are in

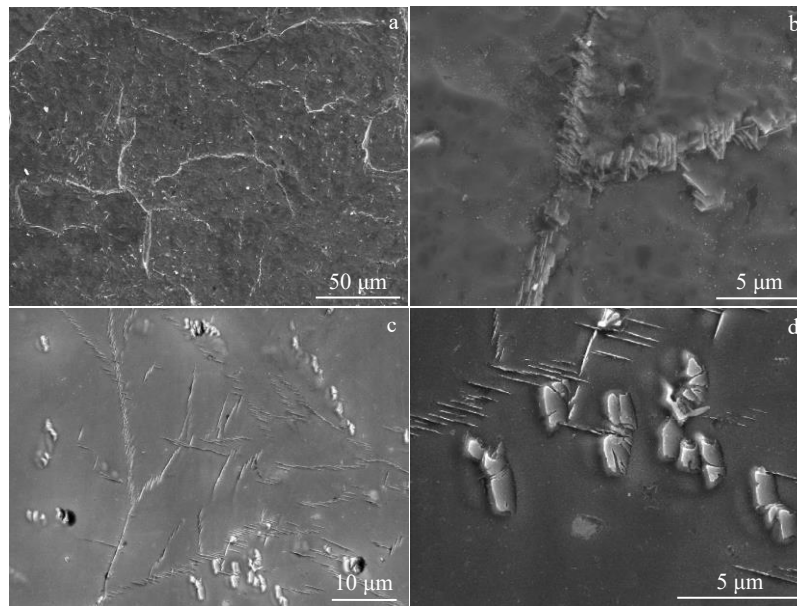


Fig.3 Microstructures and precipitates of the V-5Cr-5Ti alloy in as-cast state (a, b) and after homogenization (c, d)

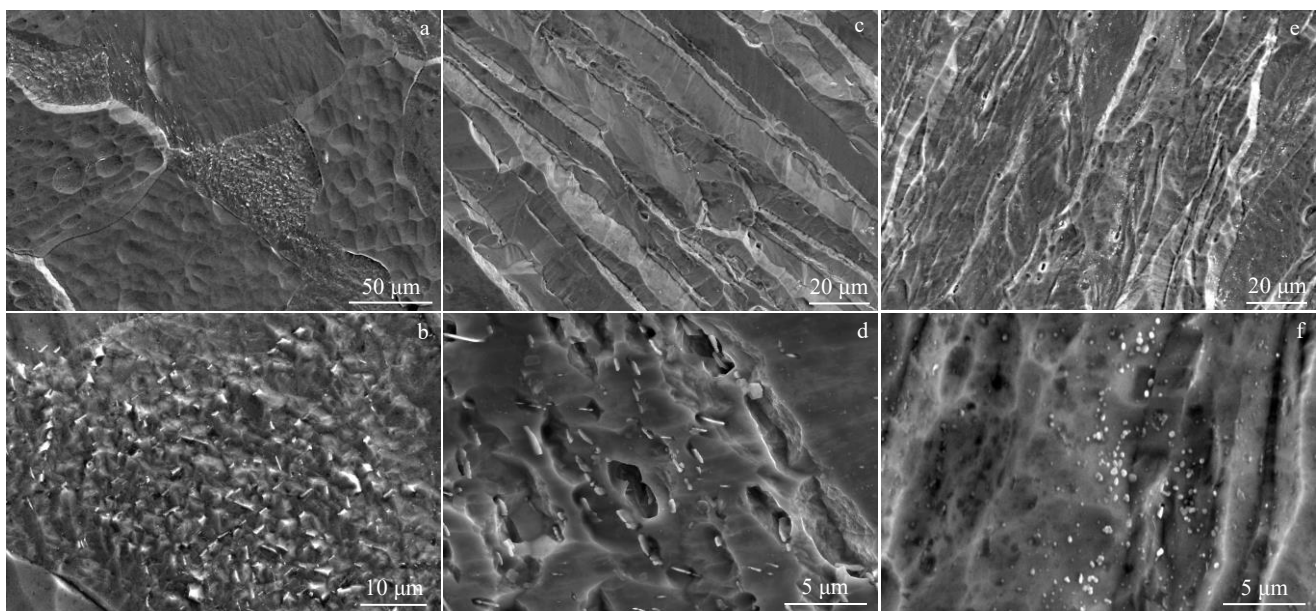


Fig.4 SEM images of microstructures and precipitates of V-5Cr-5Ti alloy after deformation processing: (a, b) hot forging+1020 °C/1 h; (c, d) 40% cold rolling; (e, f) 80% cold rolling

banded pattern, as shown in Fig. 4f. After cold rolling, the short-bar phases are broken into spherical phases.

Fig.5 exhibits the microstructures of V-5Cr-5Ti alloy after annealing at 1000 °C/1 h. The fibrous structure of 40% cold-rolling alloy disappears, with isoaxial recrystallization grains as main characteristics. However, recrystallization occurs slowly in the precipitate concentration area, because the precipitates impede the recrystallization. The recrystallization grains in this region are small (Fig.5a). The observation of the precipitate concentration area reveals that a large number of precipitates exist at the grain boundary, the number of short-bar phases is greatly reduced, and the number of granular

phases is increased. The precipitates have an uneven size and are in irregular arrangement (Fig.5b). The fibrous structure of 80% cold-rolling alloy fully disappears, with isoaxial recrystallization grains as characteristics, as shown in Fig.5c. A large number of precipitates are observed in the grain boundary, and the spherical phases have a uniform size and are dispersedly distributed in banded structures, as shown in Fig.5d.

## 2.2 Precipitate

Fig. 6 shows the precipitates and SAED patterns in V-5Cr-5Ti alloy. There are lamellar phases in as-cast alloy. During homogenization, there are needle-like phases in the alloy.



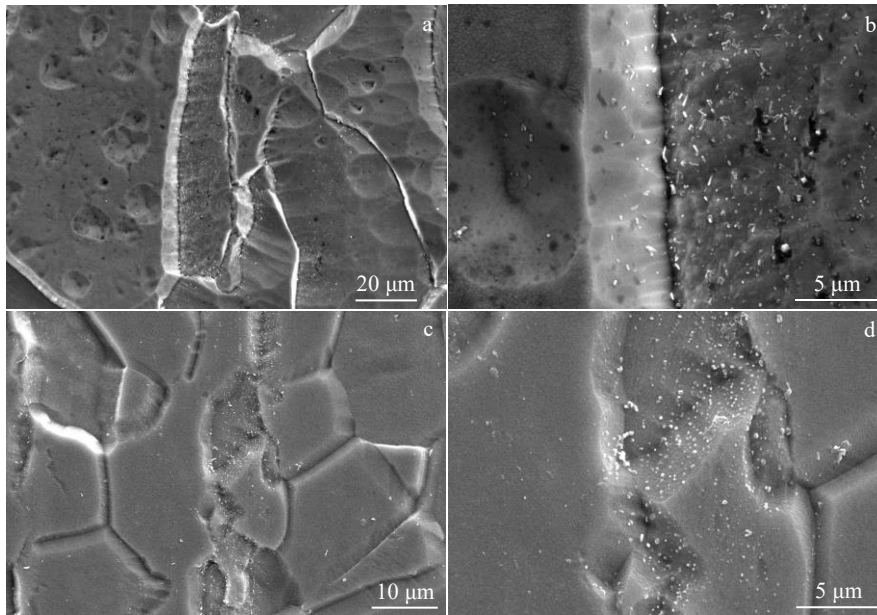


Fig.5 Microstructures and precipitates of cold-rolled V-5Cr-5Ti alloy after annealing: (a, b) 40% cold rolling+1000 °C/1 h; (c, d) 80% cold rolling+1000 °C/1 h

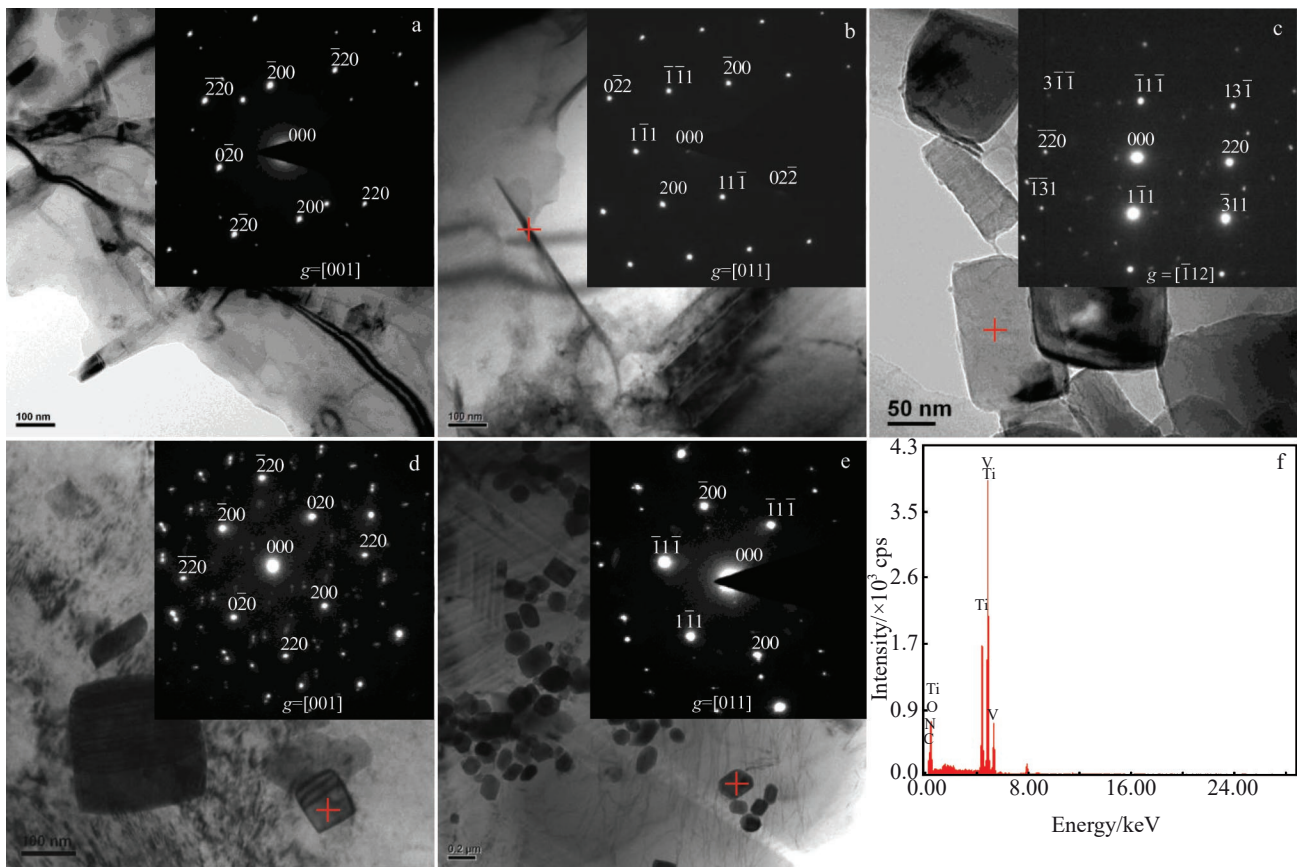


Fig.6 TEM images and SAED patterns of precipitates in V-5Cr-5Ti alloy: (a) as-cast; (b) homogenization; (c) forging+1020 °C/1 h; (d) 40% cold rolling; (e) 80% cold rolling; (f) EDS spectrum of the precipitate marked in Fig.6d

After forging, the short bar phases are found. Under deformation, the spherical phases disappear in the matrix.

Table 2 is the results of SAED and EDS analysis of the

precipitates. The results show that the precipitates are titanium oxycarbonitride, in which V and Cr elements are alloyed. They have fcc structure, and can be expressed as (TiV) (CON).

**Table 2 SAED and EDS results of the precipitates in V-5Cr-5Ti alloy**

State	V/at%	Ti/at%	Cr/at%	C/at%	O/at%	N/at%	Structure	Lattice constant/nm
As-cast	20.24	45.2	2.6	8.37	13.71	9.83	fcc	0.418~0.423
Homogenization	11.25	34.72	1.01	15.41	9.88	27.71	fcc	0.419~0.426
Forging+1020 °C/1 h	3.79	59.88	-	8.99	15.57	11.74	fcc	0.425~0.435
40% cold rolling	39.2	30.4	-	15.8	14.6	-	fcc	0.433~0.443
80% cold rolling	11.43	52.66	0.55	11.29	6.16	17.88	fcc	0.436~0.441
40% cold rolling+1000 °C/1 h	11.67	46.59	0.72	8.58	7.47	24.94	fcc	0.433~0.438
80% cold rolling+1000 °C/1 h	11.43	42.39	1.07	13.71	7.32	24.05	fcc	0.431~0.439

### 2.3 Fracture morphology

Fig. 7 illustrates the tensile fracture morphologies of the as-cast and homogenized V-5Cr-5Ti alloy. The fracture morphology is mainly characterized by cleavage steps turning into a “river” pattern, accompanied with scattered elongated dimples. After homogenization, the fracture morphology presents two characteristics: one is that there are a large number of precipitate particles and holes left by particle shedding on the grain boundary surface; the other is that there are “cleave-like” small planes, micropores and tearing edges.

Fig. 8 shows the fracture morphologies of V-5Cr-5Ti alloy after forging and cold rolling. After forging, the fracture shows a large number of equiaxial dimples, and shear planes appear locally. After 40% cold rolling, the fractures are mainly characterized by elongated dimples, and some large dimples contain several small dimples. The sliding surface is separated into undulating and curved stripes, forming a serpentine pattern. After 80% cold rolling, the fractures are mainly characterized by elliptical pits and reticular dimples. Elliptical pits are composed of a large number of dimples and have a considerably smaller depth than plastic holes. Reticular dimples are smooth and shallow at the bottom. The precipitate

is found in the dimple center.

Fig. 9 presents the fracture morphology of cold-rolling V-5Cr-5Ti alloy after annealing at 1000 °C/1 h. The fracture of the 40% cold-rolling alloy after annealing is mainly characterized by large plastic holes and equiaxial dimples. Precipitates exist in the center of the equiaxial dimple (Fig. 9b). The fracture of the 80% cold-rolling V-5Cr-5Ti alloy after annealing is mainly characterized by equiaxial dimples, and elongated dimples are distributed in a serpentine pattern. Precipitates also exist in the center of the equiaxial dimple (Fig. 9d).

### 2.4 Room-temperature tensile property

Table 3 shows the tensile test results of V-5Cr-5Ti alloy in different states at room temperature. Fig. 10 exhibits the histogram drawn from the tensile results of Table 2. The microstructure and tensile fracture morphology indicate that the dendritic structure results in high brittleness, with a minimum elongation of 5.0%. After homogenization, a needle-like dendritic structure forms, the strength and plasticity of the alloy are improved, and the average elongation reaches 17.8%. After hot forging+1020 °C/1 h, the needle-like phase is broken into a short-bar phase, the strength increases, and the elongation decreases slightly. The fracture mechanism

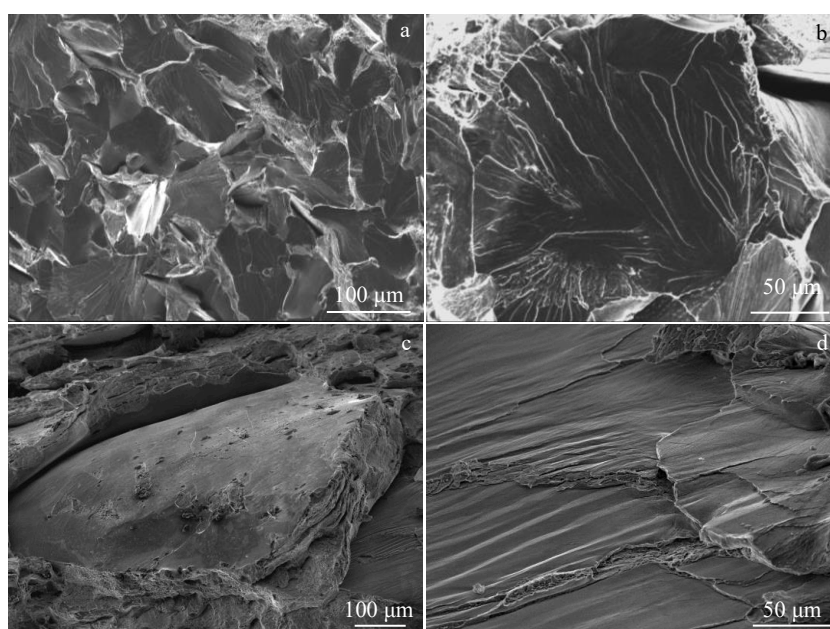


Fig. 7 Fracture morphologies of V-5Cr-5Ti alloy in as-cast state (a, b) and after homogenization (c, d)



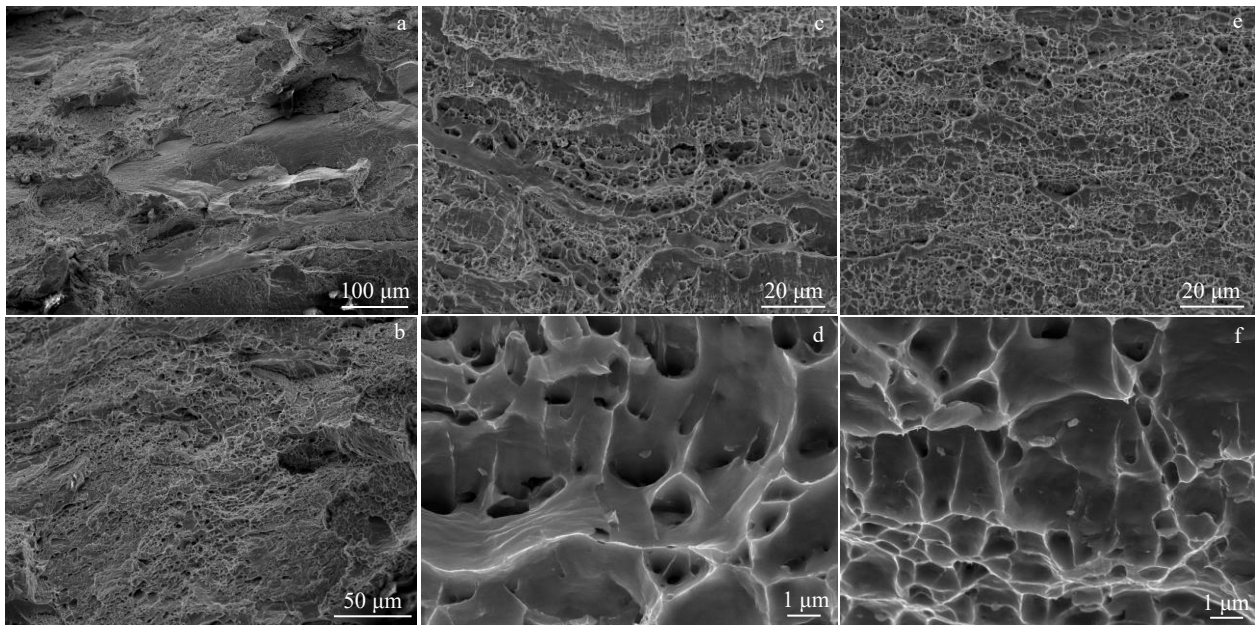


Fig.8 Fracture morphologies of V-5Cr-5Ti alloy after deformation processing: (a, b) forging+1020 °C/1 h; (c, d) 40% cold rolling; (e, f) 80% cold rolling

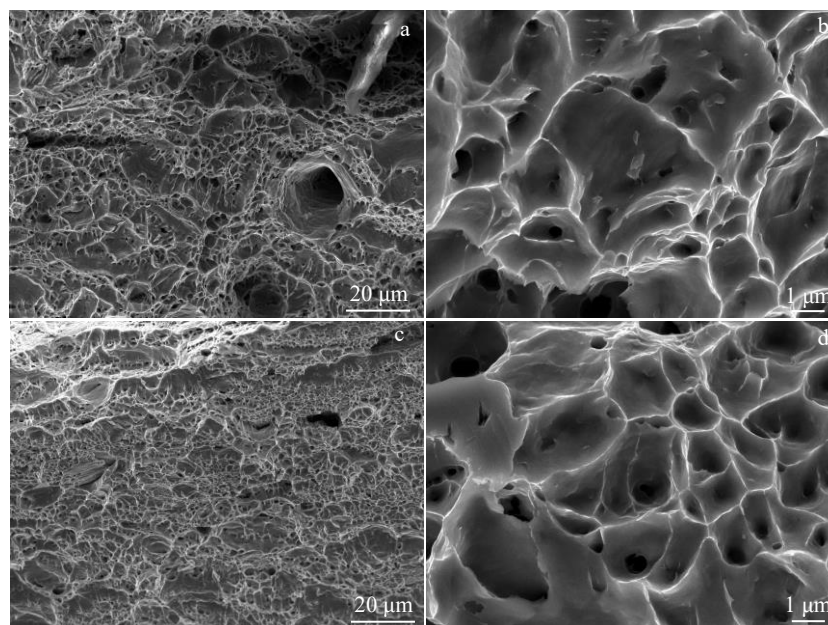


Fig.9 Fracture morphologies of cold-deformed V-5Cr-5Ti alloy after annealing: (a, b) 40% cold rolling+1000 °C/1 h; (c, d) 80% cold rolling+1000 °C/1 h

changes from a cleavage fracture of the as-cast alloy into intergranular and quasi-cleavage fractures after homogenization and then a microporosity fracture after forging.

After cold rolling, the precipitates of V-5Cr-5Ti alloy are broken into short bars or spheres, and the banded structures form. During cold rolling, slipping, dislocation, entanglement, and proliferation occur, resulting in grain elongation, fragmentation, and fibrosis. The strength increases dramatically, but the plasticity remains higher than that of the

as-cast alloy. The average tensile strength and elongation of 80% cold-rolling V-5Cr-5Ti alloy are 752.3 MPa and 8.3%, respectively. After annealing at 1000 °C/1 h, the strength decreases sharply due to recrystallization, the plasticity increases rapidly, the strength is decreased by 35.2% and the elongation is increased by 215.7%. In contrast, the strength of alloy after 40% cold rolling+1000 °C/ 1 h annealing is not significantly increased, but the elongation is sharply increased. The strength and ductility of alloy after 80% cold rolling+1000 °C/1 h annealing are improved, exhibiting

**Table 3** Tensile test results of the V-5Cr-5Ti alloy

State	Tensile strength/MPa			Yield strength/MPa			Elongation/%		
As-cast	495	475	545	405	400	440	10	5.0	9.5
	Ave.=505.0			Ave.=415.0			Ave.=8.2		
Homogenization	390	403	411	339	325	346	16.5	22.0	15.0
	Ave.=401.3			Ave.=336.7			Ave.=17.8		
Forging+1020 °C/1 h	421	473	455	348	392	374	21.5	11.5	14.5
	Ave.=449.7			Ave.=371.3			Ave.=15.8		
40% cold rolling	649	653	647	639	652	646	13	11	13
	Ave.=649.7			Ave.=645.7			Ave.=12.3		
80% cold rolling	757	752	748	755	745	745	9	8	8
	Ave.=752.3			Ave.=748.3			Ave.=8.3		
40% cold rolling+1000 °C/1 h annealing	462	463	459	314	326	311	31	34	32
	Ave.=461.3			Ave.=317.0			Ave.=32.3		
80% cold rolling+1000 °C/1 h annealing	488	486	488	382	384	382	26	23	29.5
	Ave.=487.3			Ave.=382.7			Ave.=26.2		

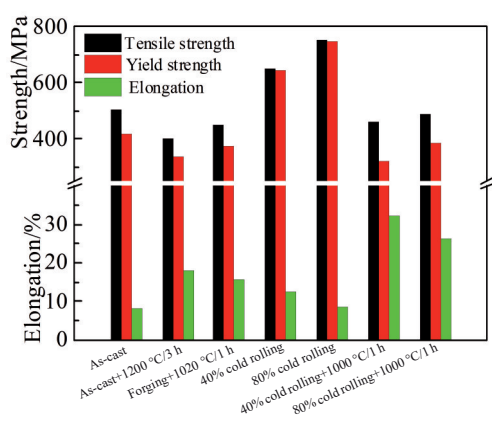


Fig. 10 Tensile properties of V-5Cr-5Ti alloy at different states

excellent comprehensive properties. The fracture mechanism of the alloy after cold rolling and annealing is microporosity fracture.

In comparison with as-cast V-5Cr-5Ti alloy, the alloy after cold rolling and annealing at 1000 °C/1 h has similar strength but considerably improved plasticity. Therefore, the dendritic structure of the precipitates deteriorates the plasticity. After 80% cold rolling, the precipitates are broken into a spherical phase. During the material deformation, the dislocation movement is blocked by the precipitates, enhancing the strength.

### 2.5 Precipitation strengthening

Fig. 11 displays the TEM images of the precipitates of V-5Cr-5Ti alloy after cold rolling. Fig. 11a presents the pin dislocation of the precipitate particles, in which the dislocation line is piled up in the precipitate particles. Fig. 11b exhibits the dislocation pileup around a single precipitate particle. Due to the addition of Cr and Ti elements, the strengthening methods of V-5Cr-5Ti alloy include solution strengthening, fine grain strengthening, dislocation strengthening, and precipitation strengthening. The

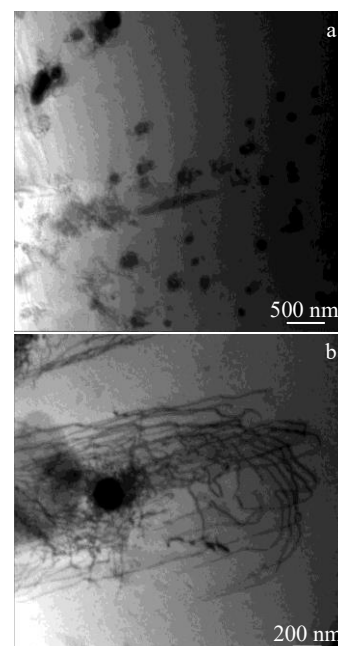


Fig. 11 TEM images of microstructures of V-5Cr-5Ti alloy after cold rolling: (a) dislocation pileup and (b) precipitate

precipitates in V-5Cr-5Ti alloy are oxycarbonitrides, which belong to the non-deformable ceramic reinforcement phase. According to the Orowan strengthening mechanism, after the moving dislocations bypass the precipitate, they will leave dislocation rings around the particle. With the increase of the number of dislocation rings, the resistance of dislocation movement increases. Therefore, the work hardening rate of Orowan strengthening mechanism is higher, and the plastic deformation can be evenly distributed in the grain.

The precipitates adopt the Orowan mechanism to strengthen the alloy matrix. The critical shear stress can be obtained using the Orowan equation<sup>[28]</sup>:

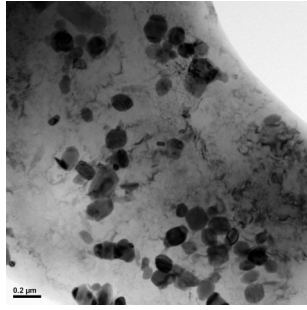


Fig.12 TEM image of precipitates in 80% cold-rolled V-5Cr-5Ti alloy

$$\tau = \frac{Gb}{\lambda} \quad (1)$$

where  $\tau$  is the critical shear stress,  $b$  is the dislocation Burgers vector,  $G$  is the shear modulus of alloy, and  $\lambda$  is the second-phase particle spacing. Eq. (1) can only simply estimate the critical shear force. The parameters in the Orowan equation need to be modified to obtain accurate intensity increment of the second-phase strengthening effect.

If the effective spacing, line tension, dislocation pair, and other influencing factors of the second-phase particles are considered, then a further accurate Orowan expression of shear stress  $\tau$  can be obtained:

$$\tau_{(\text{Orowan})} = \frac{0.81Gb}{2\pi(1-\nu)^{1/2}} \times \frac{\ln(\pi r/2b)}{r[(2\pi/3f_v)^{1/2} - \pi/2]} \quad (2)$$

On the basis of the relationship between shear and yield stresses in the reference,

$$\sigma = M\tau \quad (3)$$

the incremental expression of the yield stress generated by the Orowan mechanism is as follows:

$$\sigma_{(\text{Orowan})} = \frac{0.81MGb}{2\pi(1-\nu)^{1/2}} \times \frac{\ln(\pi r/2b)}{r[(2\pi/3f_v)^{1/2} - \pi/2]} \quad (4)$$

where  $M$  is the Taylor factor ( $M=3.1$ ),  $G$  is the shear modulus,  $\nu$  is Poisson's ratio,  $b$  is the Burgers vector,  $f_v$  is the volume fraction of the second phase, and  $r$  is the average radius of the second-phase particle.

The strengthening effect of the precipitates is calculated by using the 80% cold rolling+1000 °C/1 h annealing treated alloy as example. The interstitial atoms (C, O, N) in the alloy are supposed to form the precipitate (TiV) (CON), and the volume fraction  $f_v$  of the precipitates can be calculated with a TiC density of 4.93 g/cm<sup>3</sup> and  $f_v=0.3156\text{vol}\%$ . The size of the precipitate particles observed in Fig. 12 is 100 nm, and the average radius  $r$  is calculated to be 50 nm. On the basis of the crystal lattice constant of the V-5Cr-5Ti alloy matrix, the Burgers vector  $b$  of the alloy is 0.5260 nm. For the V-5Cr-5Ti alloy, the shear modulus  $G$  is 45.9 GPa, and Poisson's ratio  $\nu$  is 0.367<sup>[29]</sup>. These data are integrated into Eq. (4), and the increment of yield stress produced by the Orowan mechanism is calculated to be approximately 50.1 MPa.

### 3 Conclusions

1) The as-cast V-5Cr-5Ti alloy has a dendritic structure

characterized by lamellar second phase. After homogenization, the precipitates are transformed from a lamellar to a needle-like dendritic structure. The precipitates are broken into a short-bar, short-strip or spherical phase during forging and cold rolling.

2) The average tensile strength, yield strength, and elongation of the as-cast alloy are 505.0 MPa, 415.0 MPa, and 8.2%, respectively, with brittle cleavage fracture as the dominant fracture mechanism. After homogenization, the fracture mechanism is transformed into a mixed fracturing mode of intergranular and quasi-dissociative fractures. After 80% cold-rolling and 1000 °C/1 h annealing, the average tensile strength, yield strength, and elongation of the alloy are 487.3 MPa, 382.7 MPa, and 26.2%. The plasticity is greatly improved due to the morphological change in the grains and precipitates. After deformation processing, the fracture mechanism of the alloy after cold rolling and annealing is microporosity fracture.

3) During 80% cold rolling, the precipitates are broken into a spherical phase. The precipitates enhance V-5Cr-5Ti alloy by Orowan strengthening mechanism. Taking the alloy after 80% cold rolling and annealing at 1000 °C/1 h as an example, the yield strength increment obtained by precipitates strengthening is about 50.1 MPa.

### References

- 1 Muroga T, Gasparotto M, Zinkle S J. *Fusion Engineering and Design*[J], 2002(61-62): 13
- 2 Fukumoto K, Yamamoto T, Nakao N et al. *Journal of Nuclear Materials*[J], 2002, 307-311: 610
- 3 Li Ming, Song Yueqing, Cui Shun et al. *Chinese Journal of Rare Metals*[J], 2007, 31(4): 420
- 4 Fu H Y, Chen J M, Zheng P F et al. *Journal of Nuclear Materials* [J], 2013, 442(1-3): 336
- 5 Muroga T, Nagasaka T, Zheng P F et al. *Journal of Nuclear Materials*[J], 2013, 442(1-3): 354
- 6 Muroga T. *Comprehensive Nuclear Materials*[J], 2012, 189(4): 391
- 7 Takeshi Miyazawa, Takuya Nagasaka, Ryuta Kasada et al. *Journal of Nuclear Materials*[J], 2014, 455(1-3): 440
- 8 Fukumoto K, Iwasaki M, Xu Q. *Journal of Nuclear Materials* [J], 2013, 442(1-3): 360
- 9 Yan Tingxing, Yang Yitao, Ma Tongda et al. *Nuclear Techniques* [J], 2017, 40(3): 23
- 10 Krasin V P, Lyublinski I E, Soyustova S I. *Journal of Nuclear Materials*[J], 2016, 480: 40
- 11 Muroga T, Chen J M, Chernov V M et al. *Journal of Nuclear Materials*[J], 2014, 455(1-3): 263
- 12 Li Zengde, Cui Shun, Lin Chenguang et al. *Chinese Journal of Rare Metals*[J], 2007(6): 840
- 13 Xie Ruoze, Hu Wenjun, Chen Chengjun et al. *Explosion and Shock Waves*[J], 2010, 30(6): 641
- 14 Yu Yong, Pan Xiaoxia, Xie Ruoze et al. *Chinese Journal of*



- Theoretical and Applied Mechanics*[J], 2012, 44(2): 334
- 15 Wang Yarong, Zhang Yongzhi, Xu Chao et al. *Journal of Mechanical Engineering*[J], 2014, 50(10): 58
- 16 Wang Qingfu, Xian Xiaobin, Lang Dingmu et al. *Rare Metal Materials and Engineering*[J], 2012, 41(11): 2033
- 17 Li Yufei, Dong Ping, Li Ruiwen et al. *Journal of Nuclear Materials*[J], 2012, 421(1-3): 9
- 18 Zhu Boling, Yang Shanwu, Ding Jianwen et al. *Materials Letters* [J], 2015, 161: 609
- 19 Zhu Boling, Yang Shanwu, Ding Jianwen et al. *Fusion Engineering and Design*[J], 2015, 100: 171
- 20 Chen J M, Muroga T, Nagasaka T et al. *Journal of Nuclear Materials*[J], 2004, 2-3(334): 159
- 21 Chen J M, Muroga T, Qiu S Y et al. *Journal of Nuclear Materials* [J], 2004, 329-333: 401
- 22 Watanabe H, Yoshida N, Nagasaka T et al. *Journal of Nuclear Materials*[J], 2011, 417(1-3): 319
- 23 Fukumoto K, Iwasaki M. *Journal of Nuclear Materials*[J], 2014, 449: 315
- 24 Hatakeyama M, Nagasaka T, Muroga T et al. *Journal of Nuclear Materials*[J], 2013, 442: 346
- 25 Muroga T, Nagasaka T, Watanabe H et al. *Journal of Nuclear Materials*[J], 2011, 417: 310
- 26 Chen Yong, Chen Jiming, Qiu Shaoyu. *Chinese Journal of Rare Metals*[J], 2006, 30(3): 295
- 27 Nishimura A, Iwahori A, Heo N J. *Journal of Nuclear Materials* [J], 2004, 329-333: 438
- 28 Orowan E. *Symposium on Internal Stresses in Metals & Alloys* [C]. London: Institute of Metals, 1948
- 29 Harrod D L, Gold R E. *International Metals Reviews*[J], 1980, 4: 1

## V-5Cr-5Ti合金的拉伸性能及其强化机理

李增德<sup>1,2</sup>, 李卿<sup>1,2</sup>, 解浩峰<sup>1,2</sup>, 彭丽军<sup>1,2</sup>, 杨振<sup>1,2</sup>, 张文婧<sup>1,2</sup>, 黄树晖<sup>1,2</sup>, 张习敏<sup>1,2</sup>, 黄国杰<sup>1,2</sup>

(1. 有研科技集团有限公司 有色金属材料制备加工国家重点实验室, 北京 100088)

(2. 有研工程技术研究院有限公司 有色金属结构材料事业部, 北京 101104)

**摘要:** 对真空熔炼V-5Cr-5Ti合金开展了均匀化退火、热锻开坯、冷轧变形和热处理实验, 利用万能试验机、扫描电镜(SEM)和透射电镜(TEM)研究了V-5Cr-5Ti合金中析出相对力学性能影响, 估算了V-5Cr-5Ti合金中析出相强化的效果。结果表明: 铸态V-5Cr-5Ti合金存在以片层状析出相为特征的树枝状析出相, 合金均匀化退火后析出相由片层状转化为针状, 由树枝状转化成团絮状。析出相在变形过程中破碎成短条状或球状颗粒。铸态合金的抗拉强度、屈服强度和延伸率的平均值分别为505.0 MPa、415.0 MPa和8.2%, 断裂机制为脆性的解理断裂。均匀化热处理后断裂机制转变为沿晶断裂和准解理断裂共存的混合型断裂。80%冷变形+热处理后合金的抗拉强度、屈服强度和延伸率的平均值分别为487.3 MPa、382.7 MPa和26.2%, 由于晶粒及析出相形态的变化, 合金塑性得到大幅改善。锻造和冷轧后合金断裂机制为韧性的微孔型断裂。析出相以Orowan强化机制增强V-5Cr-5Ti合金, 以80%冷轧1000℃/1h退火状态合金为例, 由析出相强化获得的屈服强度增量约为50.1 MPa。

**关键词:** V-5Cr-5Ti合金; 变形加工; 析出相; 拉伸性能; 断裂机制; 析出相强化

**作者简介:** 李增德, 男, 1982年生, 博士, 教授, 有研工程技术研究院有限公司有色金属结构材料事业部, 北京 101104, 电话: 010-60662686, E-mail: lizengde@grinm.com